Behavioral Modeling of Nonlinear Power Amplifiers Using Spiking Neural Networks

Siqi Wang, Pietro Maris Ferreira, A. Benlarbi-Delai

Behavioral Modeling of Nonlinear Power Amplifiers Using Spiking Neural Networks

Siqi Wang, Pietro Maris Ferreira, Aziz Benlarbi-Delai

Sorbonne Université, CNRS, Lab. de Génie Electrique et Electronique de Paris, 75252, Paris, France
Université Paris-Saclay,CentraleSupélec,CNRS,Lab. de Génie Electrique et Electronique de Paris,91192,Gif-sur-Yvette,France

***Abstract*—In this paper, we propose a novel way for power amplifiers (PA) modeling using spiking neurons. The rate of neurons firing spikes is a nonlinear function of its excitation current. Taking the firing rate as the output and the excitation current as the input of a one layer spiking neuron network, we build up a PA behavioral model with low nonlinearity order to mimic its strong nonlinearity. The results of modeling two Doherty PA show that the proposed method can reach better performance but with lower computational complexity compared with traditional methods. This is the first time that the nonlinearity property of spiking neurons are used for processing such nonlinear signals. Future work is to develop a complete system for the training of the spiking neural networks and to explore the application of spiking neural networks on real-time PA linearization.**

***Index Terms*—Device modeling, memory effects, nonlinear distortion, power amplifiers, spiking neurons**

I. Introduction

As the third generation of neural network, the spiking neural networks (SNN) have been recently found a promising solution as they better mimic the biological behavior of the brain cortex [1]. They have been developed for conventional computers and digital signal processing circuits [2]. Recently some studies on non-von-Neumann computing hardware provide solutions to highly energy efficient SNN [3]–[5].

The SNN is usually considered as a comparable method to the classical artificial neural networks (ANN) which is less similar to the biological brain cortex, but is more developed in the past decades on von Neuman hardware [6]. The SNN is believed having over 100 times higher energy efficiency than the ANN when implementing on a field-programmable gate array (FPGA) [7]. However, the spiking neurons use can be much more variant than just composing a similar network as ANN, or even simply converting an ANN to an SNN [8]. The spiking neurons are event-driven circuits, which allows much more possibilities rather than conventional networks.

There have been different types of cortex neurons [9], such as Fast spiking neurons (FS) which fire high-frequency tonic spikes with relatively constant period, Low-threshold spiking neurons (LTS) which fire tonic spikes with pronounced spike frequency adaptation (decreasing) and rebound spikes due to post-inhibitory effect, etc. A spiking neuron fires a spike train when it is excited by a current. The rate of fired spikes f_{spike} varies as a nonlinear function of the value of the excitation current I_{ex}. Different types have different characteristics of firing rate as studied in [10].

This nonlinear characteristic of spiking neurons can offer a great practicality for nonlinear computing in information processing, such as the modeling of power amplifiers (PA) in modern telecommunication systems. The PA consumes the majority of power and brings the majority of nonlinear distortion in modern wireless communication systems [11]. Thus, developing a behavioral model of the PA is essential for the research on high efficient PA design or PA linearization. In some wideband PA linearization techniques such as [12], a digital predistortion (DPD) is employed upstream of the PA, which needs a PA model for DPD coefficients extraction. In massive multi-input multi-output (MIMO) systems for 5G, the linearization of the system with beam-forming needs to build behavioral models for each PA of the antenna array [13].

A conventional PA model is based on Volterra series [**?**]. Some simplified versions have been proposed in past decades, such as memory polynomial (MP) [14], generalized memory polynomial (GMP) [15], dynamic-deviation-reduction (DDR) model [16], and decomposed vector rotation (DVR) model [17]. Block-oriented non linear (BONL) systems [18] have also been studied. The PA distortion is composed of nonlinearity and memory effects [19]. In the Volterra based models, the nonlinearity is modeled by polynomials while the memory effects are modeled by filters.

In this paper, we use a spiking-neuron-based method to model the nonlinerity in the PA model. We mathematically analyze the nonlinear behaviors of different types of neurons and of power amplifiers from perspective of polynomials. The effectiveness of neuron-based PA model is validated with measured data from two Doherty PAs.

This paper is organized as follows. Section II presents the nonlinearity analysis of spiking neurons. The neuron-based PA modeling is proposed in Sec. III. The simulation results are given in Sec. IV. Finally, the conclusion is given in Sec. V.

II. Nonlinearity of spiking neurons

A. Model of neurons

The variations of biological current and membrane voltage in neurons are generated by passing of Sodium (Na^+) and Potassium (K^+) ions. Some models have been proposed to describe the procedure of a neuron firing spikes, such as Moris

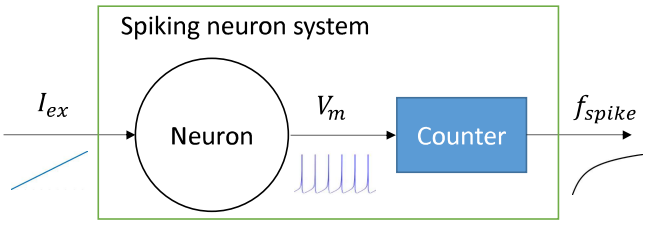

Fig. 1. A system scheme of a neuron circuit with a counter.

and Lecar (ML) model, Izhikevich model, and leaky integrate and fire (LIF) model for easier realization in hardware. In [5] and [10], the circuits of both FS and LTS neurons were designed based on ML and LIF models.

The system of a neuron circuit can be schematically illustrated as Fig 1. The variation of membrane voltage V_m as a function of excitation current I_{ex} can be described by ML model:

$$\begin{aligned} I_{ex} &= C_m\frac{dV_m}{dt} + G_{Ca}\cdot m_{SS}(V_m)\cdot(V_m - E_{Na}) \\ &\quad + G_K\cdot n\cdot(V_m - E_K) + G_L(V_m - E_L) \\ \frac{dn}{dt} &= \lambda(V_m)\cdot(n_{SS}(V_m) - n) \\ m_{SS}(V_m) &= \frac{1}{2}\left[1 + \text{Tanh}(\frac{V_m - V_1}{V_2})\right] \\ n_{SS}(V_m) &= \frac{1}{2}\left[1 + \text{Tanh}(\frac{V_m - V_3}{V_4})\right] \\ \lambda(V_m) &= \lambda_0\text{Cosh}(\frac{V_m - V_3}{2V_4}), \end{aligned} \tag{1}$$

where C_m is the membrane capacitance, G_{Ca} and G_K are maximum conductances of channels for Ca and K ions respectively, E_{Na} and E_K are Nernst potentials for Na and K ions respectively, E_L is the leakage potential, m_{SS} and n_{SS} are steady-state value of activation coefficients m and n respectively, V_1, V_2, V_3, V_4, and λ_0 are constants.

It can also be described by LIF model:

$$\begin{aligned} \frac{dV_m}{dt} &= I_{ex} + a - bV_m \\ V_m &= V_c, \text{ if } V_m > V_s \end{aligned} \tag{2}$$

where V_s is the threshold voltage to fire a spike, V_c is the rest voltage after firing a spike, a and b are constants. We can see in these models that the differential equation of membrane voltage V_m shows its gradient is negatively proportional to its own value, which means V_m increases slowly when its value is large. However, under the excitation by a current I_{ex} which is large enough, the gradient of V_m is kept positive. The membrane voltage of a neuron keeps increasing till a threshold voltage and then is abruptly reset to the rest voltage. This procedure generates a spike. With the existence of I_{ex}, the neuron keeps on generating spike train with a frequency related to the value of I_{ex}. As illustrated in Fig 1, a counter is connected to the neuron to render the spike frequency f_{spike}.

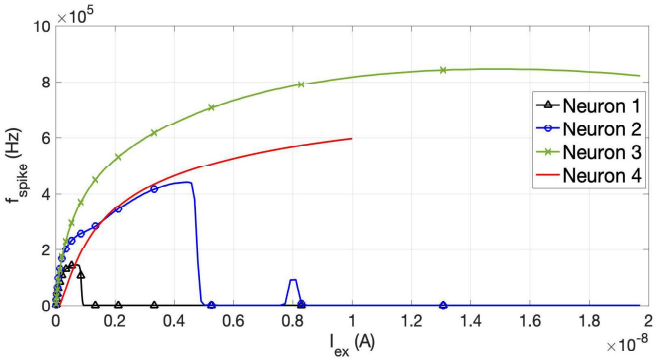

Fig. 2. Characteristics of 4 neurons.

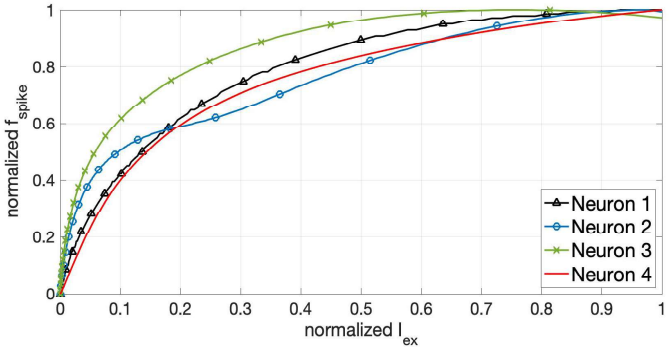

Fig. 3. Normalized characteristics of 4 neurons.

B. Nonlinear behavior of spiking neurons

The output of the system in Fig 1, the spike frequency f_{spike}, increases nonlinearly along with the value of I_{ex}. In this section, we use polynomials to model the nonlinear behavior of the spiking neurons designed in [5] and [10]. The transfer function of a neuron can be expressed by polynomials as:

$$f_{spike} = G(I_{ex}) = \sum_{j=0}^{\mathcal{J}-1}\gamma_k^{(i)}I_{ex}^j, \tag{3}$$

where $G(\cdot)$ represents the neuron function, $\mathcal{J}$ is the maximum of nonlinearity orders.

We have acquired 4 datasets from the post-layout simulations of neurons redesigned as presented in [5] and [10]:

1) Neuron 1: FS neuron with LIF model designed in [5].
2) Neuron 2: FS neuron with ML model designed in [5].
3) Neuron 3: FS neuron with ML model designed in [10].
4) Neuron 4: LTS neuron with ML model designed in [10].

The characteristics of Neuron 1-4 are illustrated in Fig 2. We are only interested in the monotone increasing parts of these curves for the PA nonlinearity behavioral modeling. Thus we limit the current I_{ex} to truncated intervals for each neuron. For better visualization, in Fig 3, the datasets of f_{spike} and I_{ex} are offset and normalized between the interval [0,1]. We can see that different types of neuron with different designs have different characteristics but with similar trends. It is wise to utilize these nonlinear response of neurons in nonlinear

TABLE I
MODELING PRECISION OF POLYNOMIALS FOR DIFFERENT NEURONS

Neuron #	1	2	3	4
$\mathcal{J}$	11	11	11	11
NMSE (dB)	-44.6	-36.8	-40.0	-54.2

devices modeling. The effectiveness of polynomial modeling is evaluated with normalized mean square error (NMSE) given in Table I. The NMSE is calculated by:

$$\text{NMSE}_i = \frac{\sum_{n=1}^{N} |y_{est}(n) - y_{meas}(n)|^2}{\sum_{n=1}^{N} |y_{meas}(n)|^2}, \tag{4}$$

where y_{est} is the estimated data obtained by the model, and y_{meas} is the measured data.

III. NEURON-BASED PA MODEL

A. The Model of PA

A conventional PA model based on memory polynomial [14] can be expressed as:

$$y(n) = \sum_{k=0}^{\mathcal{K}-1} \sum_{l=0}^{\mathcal{L}-1} c_{kl} x(n-l)|x(n-l)|^k \tag{5}$$

where $x(n)$ and $y(n)$ are PA input and output respectively, k is the nonlinearity index, l the memory index, and the c_{kl} are the complex coefficients.

As we can see in (5) that the nonlinearity of the PA is represented by $|x(n-l)|^k$. If we compare it with (3), we can easily see that the neurons can help representing high order nonlinearities in (5). Thus we propose a new model with spiking neurons to generate the nonlinearities:

$$y(n) = \sum_{k=0}^{\mathcal{K}'-1} \sum_{l=0}^{\mathcal{L}-1} c'_{kl} x(n-l) G(|x(n-l)|)^k. \tag{6}$$

In the case where we have 4 different types of neuron, we propose a combination model of 4 neurons:

$$y(n) = \sum_{i=1}^{4} \sum_{k=0}^{\mathcal{K}_i-1} \sum_{l=0}^{\mathcal{L}-1} c'_{kl} x(n-l) G_i(|x(n-l)|)^k. \tag{7}$$

where $G_i(\cdot)$ represents the function of the i-th neuron.

In case where real-time processing is not demanded, the data can be processed in low rate on neurons without parallel polyphase structure as Fig. 4(a). Note that the neurons in [5] and [10] fire spikes in order of KHz and the observation window length T is in order of 1ms, we propose to process the high-frequency data in parallel polyphase structure as illustrated in Fig. 4(b), where δt is the sampling period of original data x, P is in order of $\frac{T}{\delta t}$. Knowing that the power consumption of a neuron is in order of hundreds of pico-Watts, a dataset x sampled at several hundreds of MHz needs $P \approx 10^5$. These neurons render a total consumption of several μW, which is negligible compared to the power that the proposed method can save from traditional multiplications on digital circuits.

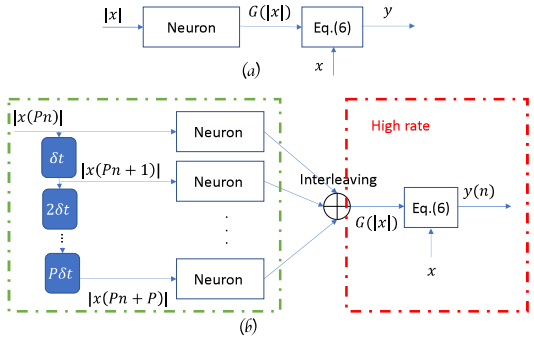

Fig. 4. (a) Structure for off-line computation; (b) Parallel polyphase structure for real-time data processing.

B. Model Identification

The identification is based on indirect learning architecture (ILA). The model coefficients can be estimated by solving a linear problem. For each band, we can express the post-distortion using matrix notation for a block of N samples:

$$\boldsymbol{y} = \boldsymbol{\Psi c} \tag{8}$$

where $\boldsymbol{y} = [y(1), \ldots, y(N)]^T$, $\boldsymbol{\Psi}$ is the $N \times R$ matrix containing the basis functions as explained in (9), and R is the total number of model coefficients.

The LS estimation of $\boldsymbol{c}$ is found by

$$\hat{\boldsymbol{c}} = [\boldsymbol{\Psi}^H \boldsymbol{\Psi}]^{-1} \boldsymbol{\Psi}^H \boldsymbol{y} \tag{10}$$

which minimizes the cost function (4).

IV. TEST RESULTS

A. Test Devices

In this section, we validate our proposed neuron-based model with datasets measured from two Doherty PAs. The PA 1 is a three-way Doherty PA with three LDMOS BLF7G22LS-130 with a linear gain of 16 dB. Its peak output power can reach 57 dBm (500 W). We use a 20 MHz LTE signal as stimulus with peak-to-average power ratio (PAPR) equal to 8 dB. Its baseband IQ signal is generated in the PC Workstation. It is then up-converted to a carrier frequency of 2.14 GHz by an Arbitrary Waveform Generator (AWG) and is fed to a driver and the PA. The AM/AM & AM/PM (Amplitude Modulation/Amplitude Modulation & Amplitude Modulation/Phase Modulation) curves of this PA are illustrated in Fig 5. The PA 2 is a two-way Doherty PA using CGHV27030S transistors. Its AM/AM & AM/PM curve is depicted in Fig 6.

B. Exhaustive Test

To investigate the effectiveness of proposed neuron-based model, we test all possible models under condition that $\mathcal{K}_i \leqslant 3$, $\mathcal{L} \leqslant 4$ in (7). The NMSE values are plotted as red points in Fig. 7 and Fig. 8 as a function of number of model coefficients R. The conventional MP models are also tested for comparison. For the conventional MP, we first test all models with $\mathcal{K} \leqslant 3$, $\mathcal{L} \leqslant 4$ and mark their results with cross symbol. We then test all conventional MP models with

$$\boldsymbol{\Psi} = \begin{bmatrix} x(n) & \cdots & x(n-L+1) & x(n)|G(x(n))| & \cdots & \cdots & x(n-L+1)|G(x(n-L+1))|^k \\ x(n-1) & \cdots & \cdots & \cdots & \cdots & \cdots & \cdots \\ \vdots & \vdots & \vdots & \vdots & \vdots & \vdots & \vdots \\ x(n-N+1) & \cdots & x(n-L-N+2) & \cdots & \cdots & \cdots & x(n-L-N+2)|G(x(n-L-N+2))|^k \end{bmatrix} \tag{9}$$

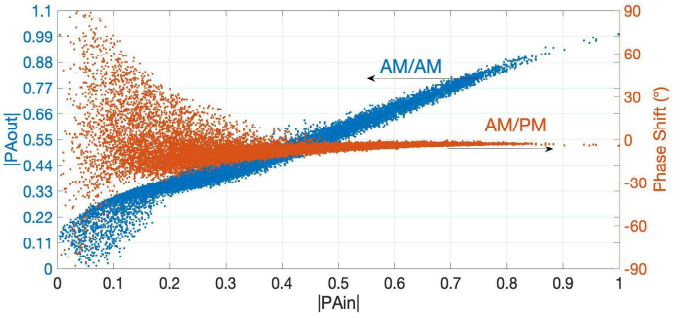

Fig. 5. AM/AM & AM/PM curve of Doherty PA 1.

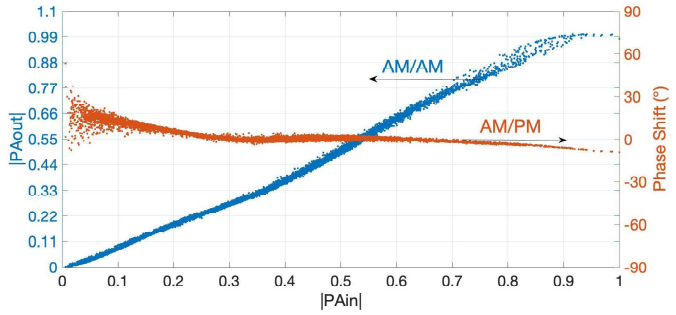

Fig. 6. AM/AM & AM/PM curve of Doherty PA 2.

$\mathcal{K} \leqslant 11$, $\mathcal{L} \leqslant 4$ and mark the corresponding results with squares. The NMSE value presents the accuracy of a model. The complexity of a model is determined by the number of its coefficients and the nonlinearity order according to [20]. It is desirable for a model to reach a low NMSE value with few coefficients and low nonlinearity order. The Pareto front of NMSE vs. number of coefficients represents the set of best models regarding the tradeoff between the NMSE value and the number of coefficients [21]. We can see that the proposed neuron-based model has a much better Pareto front than the conventional MP models. If we limit the nonlinearity order of a conventional MP model to the same as the proposed neuron-based model, the proposed neuron-based model has advantage of 5dB on NMSE. If we unlimit the nonlinearity order of the conventional MP, it can reach a similar level of NMSE as the proposed neuron-based model, but its NMSE is still 1 or 2 dB less when the number of coefficients is less than 20 for PA 1 and 15 for PA 2. This is because the neurons that we used in this paper have taken place of nonlinearities in order of 11 according to Table I. Thus we can model a high nonlinear Doherty PA with very low order in the proposed neuron-based model. We should also notice that the nonlinearity order means numerous multiplications on digital circuits, which is related to up to several milli-Watts according to [11]. The power consumption brought by neurons is then negligible. Thus, according to the way to estimate the

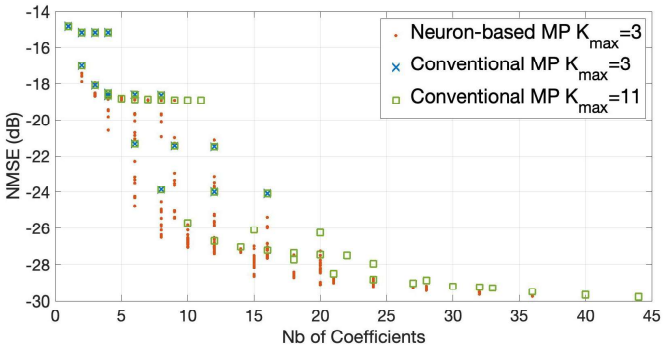

Fig. 7. Exhaustive test of NMSE for modeling of PA 1.

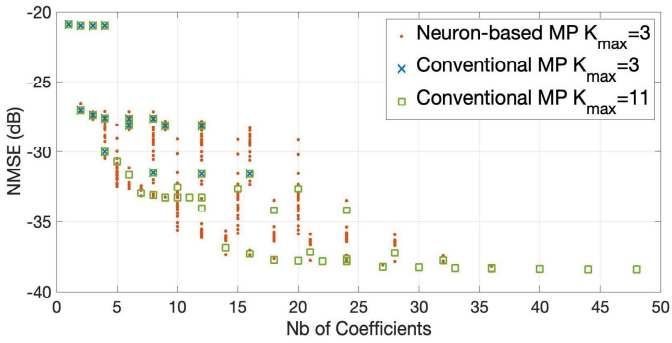

Fig. 8. Exhaustive test of NMSE for modeling of PA 2.

power consumption with FLOPs (floating-point operations per sample) in [20], the proposed model brings a reduction in order of 10 times compared with conventional method.

To the best of authors' knowledge, this is the first time that emerging techniques of spiking neurons are applied for PA nonlinearity modeling. The results show it is promising but some further development is needed to refine this technique on high frequency signal processing and real implementation. A future perspective is the design of circuits to enable the training of the spiking neural networks with some algorithms such as in [22]–[24]

V. Conclusion

In this paper, we propose a neuron-based model for PA modeling with lower complexity and power consumption. The spiking neurons with strong nonlinear characteristics help to reduce the nonlinearity order from conventional MP models, which renders less multiplications in digital computation. Furthermore, the power consumption of the spiking neurons are as low as several hundreds of pico-Watts. The utilization of new emerging techniques of spiking neurons on nonlinear device modeling has been proven effective and promising according to the validation with two different Doherty PAs.

REFERENCES

[1] W. Maass, "Networks of spiking neurons: The third generation of neural network models," *Neural Netw*, vol. 10, no. 9, pp. 1659–1671, 1997. [Online]. Available: https://www.sciencedirect.com/science/article/pii/S0893608097000117

[2] T. Matsubara and H. Torikai, "An asynchronous recurrent network of cellular automaton-based neurons and its reproduction of spiking neural network activities," *IEEE Transactions on Neural Networks and Learning Systems*, vol. 27, no. 4, pp. 836–852, 2016.

[3] R. Borwankar, A. Desai, M. R. Haider, R. Ludwig, and Y. Massoud, "An analog implementation of fitzhugh-nagumo neuron model for spiking neural networks," in *2018 16th IEEE International New Circuits and Systems Conference (NEWCAS)*, 2018, pp. 134–138.

[4] P. M. Ferreira, N. De Carvalho, G. Klisnick, and A. Benlarbi-Delai, "Energy efficient fj/spike lts e-neuron using 55-nm node," in *2019 32nd Symposium on Integrated Circuits and Systems Design (SBCCI)*, 2019, pp. 1–6.

[5] C. Loyez, K. Carpentier, I. Sourikopoulos, and F. Danneville, "Subthreshold neuromorphic devices for spiking neural networks applied to embedded a.i," in *2021 19th IEEE International New Circuits and Systems Conference (NEWCAS)*, 2021, pp. 1–4.

[6] S. Davidson and S. B. Furber, "Comparison of artificial and spiking neural networks on digital hardware," *Frontiers in Neuroscience*, vol. 15, 2021. [Online]. Available: https://www.frontiersin.org/article/10.3389/fnins.2021.651141

[7] Y. Cao, Y. Chen, and D. Khosla, "Spiking deep convolutional neural networks for energy-efficient object recognition," in *International Journal of Computer Vision*, 2015, pp. 54–66.

[8] S. Sharmin, P. Panda, S. S. Sarwar, C. Lee, W. Ponghiran, and K. Roy, "A comprehensive analysis on adversarial robustness of spiking neural networks," in *2019 International Joint Conference on Neural Networks (IJCNN)*, 2019, pp. 1–8.

[9] A. Cappy, *Neuro-inspired Information Processing*, ser. Electronics Engineering Series. Wiley-ISTE, 2020.

[10] P. M. Ferreira, J. Nebhen, G. Klisnick, and A. Benlarbi-Delai, "Neuromorphic analog spiking-modulator for audio signal processing," in *Analog Integrated Circuits and Signal Processing*, vol. 106, 2021, pp. 261–276.

[11] J. Wood, *Behavioral Modeling and Linearization of RF Power Amplifiers*, ser. Artech House Microwave Library. Artech House, 2014.

[12] Y. Liu, J. J. Yan, H.-T. Dabag, and P. M. Asbeck, "Novel technique for wideband digital predistortion of power amplifiers with an undersampling adc," *IEEE Transactions on Microwave Theory and Techniques*, vol. 62, no. 11, pp. 2604–2617, 2014.

[13] C. Yu, J. Jing, H. Shao, Z. H. Jiang, P. Yan, X.-W. Zhu, W. Hong, and A. Zhu, "Full-angle digital predistortion of 5g millimeter-wave massive mimo transmitters," *IEEE Transactions on Microwave Theory and Techniques*, vol. 67, no. 7, pp. 2847–2860, 2019.

[14] J. Kim and K. Konstantinou, "Digital predistortion of wideband signals based on power amplifier model with memory," *Electronics Letters*, vol. 37, no. 23, pp. 1417–1418, Nov 2001.

[15] D. Morgan, Z. Ma, J. Kim, M. Zierdt, and J. Pastalan, "A generalized memory polynomial model for digital predistortion of rf power amplifiers," *IEEE Trans. Signal Process.*, vol. 54, no. 10, pp. 3852–3860, Oct. 2006.

[16] A. Zhu, J. Pedro, and T. Brazil, "Dynamic deviation reduction-based volterra behavioral modeling of RF power amplifiers," *IEEE Trans. Microw. Theory Techn.*, vol. 54, no. 12, pp. 4323–4332, Dec 2006.

[17] A. Zhu, "Decomposed vector rotation-based behavioral modeling for digital predistortion of RF power amplifiers," *IEEE Trans. Microw. Theory Techn.*, vol. 63, no. 2, pp. 737–744, Feb 2015.

[18] S. Wang, M. Abi Hussein, O. Venard, and G. Baudoin, "Optimal sizing of two-stage cascaded sparse memory polynomial model for high power amplifiers linearization," *IEEE Trans. Microw. Theory Tech.*, vol. 66, no. 9, pp. 3958–3965, Sept 2018.

[19] S. Wang, M. Abi Hussein, O. Venard, and G. Baudoin, "A novel algorithm for determining the structure of digital predistortion models," *IEEE Trans. Veh. Technol*, vol. 67, no. 8, pp. 7326–7340, Aug 2018.

[20] A. S. Tehrani, H. Cao, S. Afsardoost, T. Eriksson, M. Isaksson, and C. Fager, "A comparative analysis of the complexity/accuracy tradeoff in power amplifier behavioral models," *IEEE Trans. Microw. Theory Techn.*, vol. 58, no. 6, pp. 1510–1520, June 2010.

[21] S. Wang, M. Roger, J. Sarrazin, and C. Lelandais-Perrault, "An efficient method to study the tradeoff between power amplifier efficiency and digital predistortion complexity," *IEEE Microwave and Wireless Components Letters*, vol. 29, no. 11, pp. 741–744, 2019.

[22] X. Li, W. Wang, F. Xue, and Y. Song, "Computational modeling of spiking neural network with learning rules from stdp and intrinsic plasticity," *Physica A: Statistical Mechanics and its Applications*, vol. 491, pp. 716–728, 2018. [Online]. Available: https://www.sciencedirect.com/science/article/pii/S0378437117307896

[23] L. Liang, X. Hu, L. Deng, Y. Wu, G. Li, Y. Ding, P. Li, and Y. Xie, "Exploring adversarial attack in spiking neural networks with spike-compatible gradient," *IEEE Transactions on Neural Networks and Learning Systems*, pp. 1–15, 2021.

[24] A. Zhang, X. Li, Y. Gao, and Y. Niu, "Event-driven intrinsic plasticity for spiking convolutional neural networks," *IEEE Transactions on Neural Networks and Learning Systems*, pp. 1–10, 2021.